Ocean Sci. Discuss., 12, 103–134, 2015
www.ocean-sci-discuss.net/12/103/2015/
doi:10.5194/osd-12-103-2015

Ocean Science
Discussions
Open Access

Atmosphere–ocean interactions in the Greenland Sea during solar cycles 23–24, 2002–2011

P. E. Binns

Broomlee Mains, West Linton, Edinburgh EH46 7BT, UK

Received: 5 September 2014 – Accepted: 8 January 2015 – Published: 27 January 2015

Correspondence to: P. E. Binns (pebinns@btinternet.com)

Published by Copernicus Publications on behalf of the European Geosciences Union.

Abstract

Relationships between solar activity and climate in the North Atlantic region have long been reported and, more recently, mechanisms have been proposed to explain these. Normally such relationships are tested over decadal time scales. Here, daily sea surface temperature fields bridging the period of exceptionally low solar activity between solar cycles 23 and 24 have been analysed. The day-to-day variability of the fields has been measured and the fields have been classified, using cluster analysis. The main water masses are clearly expressed, together with detail of their interactions. Three features relate to the level of solar activity. First, there is a statistically significant difference in the day-to-day variability of the sea surface temperature field between the period of lowest solar activity and the remaining periods. Second, during the transition from summer to winter, there are systematic, inter-annual changes in the day-to-day variability of the sea surface temperature field. Third, the forms of the late summer temperature fields exhibit symmetry about the years of lowest solar activity. These features are attributable to variability in the passage of weather systems. The influence on North Atlantic surface climate of variations in the solar ultraviolet band acting through the stratosphere has been reported in a number of studies. This provides a credible mechanism for solar activity influencing sea surface temperatures in the Greenland Sea.

1 Introduction

The Nordic Seas, including the Greenland Sea, have long been a focus of interest, due to the exchanges which take place there between the atmosphere and the ocean currents which flow through them (Fig. 1). Atmosphere–ocean interactions in these seas are important because cooling and sinking of the waters in the area contribute to the North Atlantic thermohaline circulation, and thus have an influence beyond the area. Recent work has described relationships between solar activity and North Atlantic climate and proposed mechanisms to explain these (Gray et al., 2010). Normally such relationships are tested over decadal time scales. However, the exceptional length and depth of the solar low between Cycles 23 (peaking in 2000–2002) and 24 (with an initial peak in 2011), together with the availability of daily sea surface temperature grids, offer the opportunity for a different perspective on these relationships. From June 2006 to August 2010, monthly Wolf Sunspot Numbers were consistently below 20, and from June 2007 to November 2009 they were consistently below 10 (NOAA, 2011). A set of consistent, daily sea surface temperature (SST) data is available from June 2002 to September 2011, conveniently spanning the solar low. Apart from any link with solar activity, detailed understanding of atmosphere–ocean interactions is important if they are to be represented accurately in climate models. Short-lived events are not captured by climate models with low resolution and description at this high level of temporal and spatial resolution provides important new information. The high spatial and temporal resolution also provides new information about interactions between the main water masses. The main objective of this study is, therefore, to test whether there is a significant relationship between changes in the SST field and solar activity during the extreme solar low between cycles 23 and 24.

2 Data and methods

2.1 AVHRR-AMSR sea surface temperature data

Between June 2002 and September 2011 the combination of the Advanced Very High Resolution Radiometer (AVHRR) with the Advanced Microwave Scanning Radiometer (AMSR) increased coverage of SSTs and a set of daily grids, with consistent acquisition and processing, is the basis for this study (NASA, 2015). Version 2 of these data has been used. They have been calibrated against in situ data from ships, buoys and sea ice concentrations, using an "optimum interpolation" technique to produce a daily grid with a resolution of 0.25° of latitude and longitude (Reynolds and Smith, 1994;

OSD
12, 103–134, 2015

Reynolds et al., 2007). The AMSR data may be contaminated during precipitation and within 75 km of land and ice (Reynolds et al., 2007; Høyer et al., 2012). The data used here lie outside areas within 75 km of land but the data may be contaminated by precipitation. The presence of ice is taken into account in processing the data. The processing algorithms are designed to minimize the effects of atmospheric water vapour and to convert the measurements to represent SSTs to a water depth of 0.5 m. The Jan Mayen volcano, 300 km to the southwest, has not erupted during the period and is unlikely to have produced aerosols (GWP, 2014; Imsland, 1986). Mean temperatures have been calculated taking into account the progressive northward reduction in area represented by the grid points. Unlike absolute temperatures or temperature anomalies, day-to-day variability is naturally less susceptible to errors caused by longer term biases in satellite measurements.The data set starts in June, and the analyses are based on annual periods running from June to May; this has the advantage that the critical transitions from summer to winter are centralised. Unconventionally, the sea surface temperature fields are shown as viewed from the north and displayed as isometric plots; this improves visibility of detail in the northward sloping temperature fields.

2.2 Classification of sea surface temperature fields and day-to-day variability

The 3409 daily SST fields have been classified using cluster analysis a multivariant statistical technique which groups "objects" (here the SST fields) based on measurements made on them (Appendix A, Everitt, 1977; Trauth, 2007). Two sets of cluster analyses were made (Fig. 2, Supplement p. 2–3): (1) twelve runs, one for each month of the year (the "monthly analyses"); e.g. an analysis would comprise all Junes from June 2002 to June 2011; (2) nine annual runs starting with June 2002 to May 2003 and ending with June 2010 to May 2011 (the "annual analyses"). These analyses enabled sequences of days with similar SST fields to be assigned to a cluster and recognised in other months or years. Mean SST fields for the days in a cluster have been calculated.

A by-product of the clustering process is the euclidean distance in multi-dimensional space between two days. Here this is taken as a measure of the difference between

OSD
12, 103–134, 2015

the SST fields on successive days and is referred to hereafter as “day-to-day variability” or “variability”. Whilst the unit of variability is temperature, once this is translated into euclidean distance in multi-dimensional space, the values only have a meaning relative to each other. When defining clusters, euclidean distances were arbitrarily selected as cutoffs to give a manageable number of clusters. Variability is summarised as monthly and annual averages, providing a measure of the seasonal and annual variability of the SST field.

2.3 Analysis of weather systems interpreted from infra-red satellite images

The more common approach to tracking weather systems, in particular cyclones, is to apply some form of search algorithm to sequential atmospheric pressure fields. The time scales in this study, however, are short enough to allow visual interpretation of satellite images, and hence a more detailed description. Smaller scale cyclones are identified as well as systems advecting cold polar air southwards. The shorter term atmospheric movements, associated with weather systems, has been examined here in a detailed study of thermal infrared satellite images (10.3–11.3 µm), extending from summer though to winter in two contrasting periods, 2004–2005 and 2008–2009 (NERC, 2013). Weather systems, imaged in at least twelve passes a day, have been recognised by characteristic cloud formations and recorded. This enabled the variable passage of weather systems and cold air outbreaks to be compared with variations in the daily SST fields.

3 Oceanographic and atmospheric setting

3.1 Bathymetry, hydrography, geology

The Greenland Sea, lying between Greenland and Svalbard, narrows northwards into the Fram Strait (Fig. 1) (NOAA, 2012). Water depths increase northward and exceed 5500 m, before shallowing up to a sill between 2400 and 2600 m in the Fram Strait. The

OSD
12, 103–134, 2015

principle bathymetric features are the Knipovich Ridge, an ocean spreading centre, and its associated transform fault zones. Circulation in the Nordic Seas is dominantly barotropic and controlled by the bathymetry (Voet et al., 2010).

The warm, saline water of the West Spitsbergen Current (WSC) carries heat northwards and is modified by losing heat to the atmosphere, by freezing and by the influx of fresh water from runoff and precipitation. In the Fram Strait the WSC branches (Schauer et al., 2008). Two branches continue into the Arctic Ocean and the third turns westward and southward as recirculating Atlantic Water (RAW) to converge with Polar Water (PW) flowing southward out of the Arctic Ocean, into the East Greenland Current (EGC). Whilst convective transformation of the water masses mostly takes place in basins such as the Greenland Sea, the transformed water is exported via edge currents such as the EGC to contribute to the North Atlantic Deep Water (Latarius and Quadfasel, 2010).

3.2 Atmosphere and ocean

The dominant regional mode of atmospheric variability is represented by the relative sea level pressures in the areas of the Azores and Iceland, as quantified by the North Atlantic Oscillation index (NAO) (Wanner et al., 2001; Hurrell et al., 2003; Hurrell and Deser, 2009). However, changes in the configuration of the regional pressure field, for example variations in the main centres of pressure, may produce local changes. Visbeck et al. (2003) point out the difficulty in ascribing a given feature of SSTs to the NAO, as the ocean responds on time scales ranging from days to decades, and the response is dependent on various mechanisms. These have been attributed variously to internal processes within the troposphere, to events in the stratosphere propagating downwards, and to low-frequency changes in the ocean (Furevik and Nilsen, 2005).

Precipitation in the Greenland Sea reaches a maximum in the autumn. At 74° N, in the south of the study area, the boreal night starts in October and continues through to February. Apart from the movement of heat and moisture northwards by AW, the climate is dominated by weather systems which range both in scale and type (Harold

OSD
12, 103–134, 2015

et al., 1999a, b; Sorteberg and Walsh, 2008; Blechschmidt et al., 2009; Noer et al., 2011). Synoptic-scale systems, often originating in the south may generate less intense, meso-scale cyclones. There are also periods when cold polar air masses advect southwards over the warmer waters (“cold air outbreaks”) (Kolstad et al., 2009). These may generate small-scale cyclones, distinctive linear cloud patterns (cloud streets) and fog.

3.3 Monthly mean sea surface temperatures

Mean SSTs over the area are influenced both by the AW and PW inflows, as well as by seasonal changes in irradiance and interaction with the atmosphere. Mean summer SSTs in the area increased from 2003 to 2006–2007, before decreasing in 2008 to increase again in 2009 (Fig. 3). The increase in SSTs over the West Spitsbergen sector up to 2006–2007 is consistent with measurements of the mean temperature of the total AW inflow measured at moorings along 78°50′ N (Timmermans et al., 2012). The winter minima for the whole area increased by $\sim 0.8^{\circ}$ from 2002–2003 to 2006–2007, before decreasing in 2007–2008 and 2008–2009. This is consistent with the increased flow of ice out through the Fram Strait in the latter years (Smedsrud et al., 2011). SSTs of the individual sectors track each other, with the exception of the northwest sector, where the inflow of PW influences temperatures.

4 The sea surface temperature fields

4.1 The main water masses

The warm waters of the WSC and the RAW, together with the cold PW are apparent on the SST fields (Fig. 2). As autumn gives way to winter there is an exceptional seasonal change in SSTs in the southwest; SSTs progressively drop to the level of PW in the northwest. In winter, therefore, there is little difference in SST between the southwest and northwest. In summer, however, SSTs in the southwest are significantly higher

OSD
12, 103–134, 2015

than those in the northwest; a steep SST gradient separates the two water masses and the warm RAW is only apparent as slightly raised "rim".

4.2 Interaction between Recirculating Atlantic Water and Polar Water

Oceanographic studies (e.g. Rudels et al., 2004) show the interaction between RAW and PW to be complex. Sections across the Fram Strait depict the less dense PW overlying RAW (Schauer et al., 2008). However, between 78 and 81° N, eddies on scales of 20–40 km are described (Johannessen et al., 1987; Gascard et al., 1995). These may be stationary or move with the current.

The SST field in the northwest as imaged by the AVHRR-AMSR data is highly variable (Fig. 4). During some periods, lasting one or more days, the warmer, southwest-trending, recirculating water forms a distinct unit with the colder PW on either side (Fig. 4a); at other times linear, west-trending features dominate (Fig. 4c); or the two may intersect, with the west-trending features appearing to interfer with the RAW (Fig. 4b). These west-trending features on the SST fields are interpreted here to be poorly-resolved expressions of eddies. They are particularly pronounced in winter, when they appear to extrude into the colder PW, consistent with a complex movement of meso-scale eddies.

5 Day-to-day variability of the sea surface temperature field

Taken together, three observations indicate a relationship between the level of solar activity and the day-to-day variability of the SST field in the Greenland Sea. First: the lowest variability coincides with the period of lowest solar activity. The statistical significance of this is established in Sect. 5.1. Second: the timing and character of the changes in variability during the transition from summer to winter varies with the level of solar activity (Sect. 5.2). Third: the forms of the late summer SST fields during the period of lowest solar activity are unique to this period, whereas those in the years

OSD
12, 103–134, 2015
Atmosphere–ocean interactions in the Greenland Sea
P. E. Binns

before and after are similar, forming an apparent symmetry about the low solar years (Sect. 5.3).

Are the features seen on the SST fields real or artefacts? The day-to-day variability of the SST field and its relationship with activity in the atmosphere may be interpreted in several ways: (1) solely due to the direct influence of the atmosphere on the sea surface; for example the exchanges of heat with advecting air masses or variations in cloud cover, (2) a combination of direct influence of the atmosphere and changes in water masses stimulated by interaction with atmosphere; for example ice movement or wind-generated turbulence or upwelling, (3) the effect of precipitation on the AMSR signal and the interpolation process, (4) some common effect; for example solar activity affecting both atmospheric conditions and the AVHRR-AMSR signals. It has long been recognised that, over short periods, the atmosphere forces the ocean and the seasonal changes in variability observed here are consistent with this; in all years, variability increases as summer gives way to autumn and winter. More significantly, the variability of the SST field is consistent with independent atmospheric pressure measurements from the onshore meteorological station at Svalbard Lufthavn (Supplement p. 4). Taking the seasons individually to avoid seasonal influence on correlation, the correlation coefficients are: MAM: 0.65; JJA: 0.07; SON: 0.49; DJF: 0.56. These observations give confidence that the day-to-day variability described here is real and not an artefact.

5.1 The coincidence of low sea surface temperature variability with the solar low

Visually, the period of lowest day-to-day variability appears to coincide with the period of exceptionally low solar activity (SSN < 10) (Fig. 5). Furthermore, between 2006 and 2008 both the winter and spring extremes decrease, paralleling the decrease in solar activity (Fig. 5b). Variability then levels off to increase again in 2010. It is critical to establish whether there is a statistically significant difference in variability between the period of low solar variability and the periods before and after (Fig. 6). Daily SST variability values were therefore divided into two groups, with the objective of testing

Discussion Paper | Discussion Paper | Discussion Paper | Discussion Paper |
OSD
12, 103–134, 2015
Atmosphere–ocean interactions in the Greenland Sea
P. E. Binns

whether there was a statistically significant difference between periods with SSNs below 10 (884 values) and the remaining periods (2525 values) (Supplement, p. 4–5). As the frequency distributions of the two groups of days are not normally distributed, both standard *t* tests and a non-parametric test, the Kolmogorov–Smirnov test, have been made. Before testing for a difference between these two groups, a set of ten reference tests was made. In each of these tests, two groups were randomly selected from the total population of day-to-day variabilities and a *t* test and a Kolmogorov–Smirnov test were run on each pair. Of these ten tests, nine supported the null hypothesis that there was no significant difference between these two, randomly-selected groups. In contrast, when the standard *t* test and the Kolmogorov–Smirnov test were made on groups taken from periods with SSNs above and below 10, statistical significance was confirmed at the 5 % level.

5.2 Interannual variability during the transition from summer to winter

5.2.1 Systematic changes in variability during July and August

The timing and character of the changes in variability during the transition from summer to winter varies according to the level of solar activity (Fig. 7a). From 2002–2006 and again in 2009 and 2010, there is a "precursor" peak in variability in July–August. This peak is pronounced in 2002, 2003 and 2004, but less so in 2005 and 2006; it is virtually absent during the years with very low solar activity, before re-appearing in 2009 and 2010.

5.2.2 Systematic changes in the timing of the autumn increase in variability

As summer gives way to winter, the steady increase in mean monthly variability tracks decreasing mean monthly temperature for four-six months (Fig. 7b–j). Tracking ceases when variability drops sharply and SSTs remain low. The period, during which the two monthly means track, changes systematically from year to year. In 2002, tracking starts

OSD
12, 103–134, 2015

in November whereas in 2008 and 2009 it starts in August; in 2010 it again starts later. These monthly means are made up of the daily values and it is necessary to confirm these interannual changes at this level of detail (Supplement, p. 6). The trends on the daily plots are naturally more irregular but the precursor and the timing of the start of the tracking are recognisable. Furthermore, the plots covering the years of the solar low (2007–2009) share a similar character with a sudden step in the level of variability in August–September.

5.3 August and September sea surface temperature fields

Some August SST fields, as classified by cluster analysis, are unique to the years of lowest solar activity; others are detected only in the years before and after, thus indicating symmetry about the period of lowest solar activity (Fig. 8a and b; Supplement p. 7–8). For September, this symmetry is present but less apparent. The causes of this symmetry have been investigated with difference plots (Fig. 8c) (Supplement p. 9–11). August SST fields during the solar low are significantly different from those before and after. Mean SSTs of the fields are lower, and SSTs in the zone of interaction between RAW and PW are significantly (2–3 °C) lower. This zone is made up of the E-W orientated features, interpreted as eddies, implying these warmer water features did not extend so far west in 2008. There is little difference between SST fields before and after the solar low.

6 Attribution

6.1 Variability of the sea surface temperature field and the North Atlantic Oscillation

The most likely cause of the day-to-day variability of the SST field is the passage of weather systems and there is support for this from the relationship between the SST variability and the NAO index (Supplement p. 12–13). Many studies have related long

Discussion Paper | Discussion Paper | Discussion Paper | Discussion Paper |

OSD

12, 103–134, 2015

Atmosphere–ocean interactions in the Greenland Sea

P. E. Binns

term changes in the ocean properties of the Nordic Seas to the NAO index (Furevik and Nilsen, 2005; Sorteberg and Walsh, 2008; Visbeck et al., 2003; Sorteberg et al., 2005). Correlations between the NAO index and the variability of the SST field vary. Over the whole period there is no clear correlation. However, over the period of low solar activity from July 2007 to November 2009, the correlation coefficient is 42 % ($P \leq 0.01$); taking only the period of lowest solar activity from October 2007 to September 2008 this increases to 89 % ($P \leq 0.01$). Taking the winter months only (December, January, February) the correlation coefficient is 54 % ($P \leq 0.01$).

6.2 Variability and weather systems

In long term studies, weather systems are identified and tracked using algorithms based on sea level pressures. The shorter time scale of this study allows detailed descriptions of weather systems within the area, as interpreted from characteristic cloud signatures on infrared satellite images (NERC, 2013). (Supplement p. 14–15). For two contrasting summer-winter transitions (July 2004 to February 2005, and July 2008 to February 2009) weather systems have been recorded in detail and compared with the variability of the SST fields (Fig. 9). These periods represent contrasting transitions from summer to winter in years with relatively high and extremely low solar activity. Whilst this is a qualitative, descriptive approach, it enables cold air outbreaks and smaller, short-lived cyclones to be identified; not just regional and meso-scale cyclonic systems as detected by automated, pressure-tracking algorithms.

There are at least ten satellite passes each day over the two periods and cloud signatures have been classified into those indicative of cyclones and those indicative of cold air outbreaks (Fig. 9; Supplement p. 16). The former have been further subdivided into the direction of origin. Systems coinciding with days associated with high variability values (> 15) have been distinguished from those coinciding with lower variability. Taking the two summer-winter transitions together, 74 % of the days with high variability coincide with the passage of cyclones. The number of cyclonic systems in 2004–2005 (79) exceeds that in 2008–2009 (62). In both periods most, but not all, the systems

OSD
12, 103–134, 2015

advected into the area from the south. Other systems originated north of the area or within the area; in some cases the origin was unclear. Conversely, there were days when cyclones were interpreted, but variability was low. There are more of such days in the 2008–2009 (27) than in 2004–2005 (17), and most of these occurred between December 2008 and February 2009, the deepest part of the solar low. In 60 % of these cases the systems were short–lived or peripheral to the area. In a further third of the cases, however, the systems were of regional extent and appeared to be no less significant than systems associated with high variabilities. An explanation may lie in the altitude of these latter systems. This has not been determined although, in a number of cases, a system can be demonstrated to lie above lower clouds and therefore not in contact with the sea surface (Fig. 10). There were also days when variability values were high and there was no cyclone activity. More than half of these days were in winter and, in two thirds of these cases, the difference fields show changes in the area of interaction between warm RAW and PW, indicating that variability of the SST field was due to ice movement, possibly due to wind, but not directly due to weather systems.

These observations suggest that high day-to-day variability of the SST field is strongly associated with high cyclone activity, with ice movement in the northwest being a secondary factor. It follows, therefore, that the systematic, inter-annual changes in SST variability during the transition from summer to winter, observed as solar activity declines, is also due to variable interaction with the atmosphere. It implies interannual differences in weather systems during autumn and early winter. This is consistent with known changes in the NAO centres of action and its spatial structure.

6.3 Variability and the interaction between Recirculating Atlantic Water and Polar Water

The apparent symmetry of the form of the August and September SST fields about the years of the solar low, is caused by significant changes in the northwest (Fig. 8c; Supplement p. 7–11). In this area, warm RAW interacts with PW. The winter of 2008 was unique in that temperatures in this sector were the lowest of all the years in this

OSD
12, 103–134, 2015

study and that sub-zero SSTs extended further to the south and east than in earlier or later years. Ice flux through the Fram Strait, has both a current and a wind-driven component, with a minimum flux in autumn increasing to a maximum in spring (Serreze and Barry, 2005). This indicates an association with variations in wind-driven sea ice. Although studies based on sea level pressure data found no relationship between ice flux through the Fram Strait and the NAO an alternative system has been proposed (Tsukernik et al., 2009; Angelen et al., 2011). Both observations and models indicate a pressure gradient, caused by a local thermal gradient between cold air in the east and warm air in the west, which drives a northerly wind and hence increase ice export.

7 Discussion

The Greenland Sea and the atmosphere interacting with it are parts of a complex system, rich in feedbacks with varying response times. Atmospheric teleconnections extend to the Mediterranean and the Pacific (Ineson and Scaife, 2009). A link to solar activity has implications for the predictability of the climate and hydrography of the Greenland Sea and beyond. For example, Condron and Renfew (2012) report simulations showing that the integrated effect of meso-scale weather systems influences deep convection. Small changes in SSTs in this area may, therefore, have a wider impact through their effect on the North Atlantic thermohaline circulation. The data presented in this study suggest that the SST field in the Greenland Sea is influenced by solar activity. If this is so, then there should be a credible explanation of the physical processes linking solar activity to the passage of weather systems and the day-to-day variability of the SST field. Such links are mostly discussed in the context of the NAO. However, Haigh et al. (2010) and Ineson et al. (2011) make a connection between solar-influenced anomalies in the stratosphere, which propagate down into the troposphere, and changes in the position of storm tracks.

Relationships between cyclone frequency and the NAO are reported for the area of the Icelandic Low by Serreze and Barry (2005), and for the Nordic Seas immediately to

OSD
12, 103–134, 2015

the south of the area studied here by Sorteberg et al. (2005). Hurrell and Deser (2009) also note that changes in the circulation patterns over the North Atlantic, associated with the NAO, relate to the number and intensity of storms and their tracks. Winters with higher NAO indices have more frequent and intensive storms in the Norwegian Sea.

In a major review of the influence of solar activity on climate, Gray et al. (2010) note studies providing evidence of the modulation of the NAO by the state of the stratosphere. These studies, on varying time scales, also propose processes. Kodera (2002, 2003) reports a solar influence on the NAO, based on 100 years of historical data. In winters during periods of low solar activity, the NAO pressure pattern is confined to the North Atlantic area. In contrast, in winters during years with high solar activity, the pattern has a much wider, hemispherical extent. Kodera (2002, 2003) notes that this is consistent with a stratospheric involvement, through the downward propagation of stratospheric zonal wind anomalies. Kodera and Kuroda (2005) further investigate the processes and suggest that the influence of solar activity originates in the stratopause, where zonal winds vary inter-annually with solar activity.

These observations have been supported by simulations and by new observations. The strengthening of the NAO in recent decades has been successfully simulated by introducing observed trends in the lower stratosphere (Scaife et al., 2005). A process connecting solar activity with the stratosphere is proposed by Ineson et al. (2011). They note that recent measurements of solar ultraviolet irradiance suggest that variations in this band are larger than previously thought. Part of the ultraviolet band contributes to solar heating, through ozone absorption in the middle atmosphere. Based on both observations and simulations, Ineson et al. (2011) show a decrease in temperature from solar maximum to solar minimum. This is attributed to the decrease in ozone heating associated with changes in ultraviolet irradiance. As this affect is greatest in the tropics, the poleward temperature gradient is thus reduced during low solar activity. These changes in the stratosphere propagate down into the troposphere. The system, however, is complicated by teleconnections (Ineson and Scaife, 2009), lags due to the

OSD
12, 103–134, 2015

long term “memory” held in ocean heat (Scaife et al., 2013) and internal, non-linear dynamics of the atmosphere (Hurrell and Deser, 2009).

The influence on North Atlantic surface climate of variations in the solar ultraviolet band acting through the stratosphere provides a credible explanation for the observations in this study and has been reported by other authors (Kuroda et al., 2008; Haigh et al., 2010; Reichler et al., 2012). The results of these studies are consistent with there being a relationship between the level of solar activity and SST variability in the Greenland Sea.

Appendix A: Cluster analysis

Cluster Analysis is a multivariant statistical technique which groups “objects” based on a series of measurements made on them (Everitt, 1974; Trauth, 2007). Here the “objects” are the daily SST fields and the measurements are the SSTs at the individual grid points. Grouping of the daily SST fields into clusters is a stepwise process, based on some measure of similarity. Here this is euclidean distance in multi-dimensional space between two points, representing two SST fields. In the hierarchical method of clustering the two points, which are closest together in this space, are found and a new point is created midway between them (average linkage method). This process is repeated until all points have been assigned to a group. The clustering process is represented graphically by a dendrogram (Fig. A1).

The distance between two points in euclidean space is used here as a measure of day-to-day variability of the SST fields. Whilst the unit of variability is temperature, once this is translated into euclidean distance in multi-dimensional space, the values only have a meaning relative to each other. When defining clusters, euclidean distances were arbitrarily selected as cutoffs to give a manageable number of clusters.

Whilst this has proved a powerful method of finding order in large, complex data sets, a potential disadvantage arises from the likely similarity of many SST fields. These can be expected to plot as a continuous cloud of points, with varying density, in multi-

OSD
12, 103–134, 2015

dimensional space. It is possible, therefore, that intermediate points lying between two dense "clouds", cause the two clouds to be joined at a lower level than they actually are. This process is called chaining. However, visual comparison of the mean SST fields produced by cluster analysis suggests that the process is providing realistic classifications. Two further results support this. First, 78 % of the cluster boundaries produced by the monthly analyses coincide with those in the annual analyses. Second, the cophenetic correlation coefficients all exceed 70 %. These coefficients measure the accuracy with which a dendrogram represents the distances between actual data points.

The Supplement related to this article is available online at doi:10.5194/osd-12-103-2015-supplement.

Acknowledgements. An earlier version of this paper benefited considerably from comments from John Huthnance.

References

Blechschmidt, A.-M., Bakan, S., and Graßl, H.: Large-scale atmospheric circulation patterns during polar low events over the Nordic Seas, J. Geophys. Res., 114, D06115, doi:10.1029/2008JD010865, 2009.

Condron, A. and Renfrew, I. A.: The impact of polar mesoscale storms on northeast Atlantic Ocean circulation, Nat. Geosci., 6, 34–37, doi:10.1038/NGEO1661, 2012.

Everitt, B.: Cluster Analysis, Social Science Research Council, Heinemann Educational Books Ltd, 1977.

Furevik, T. and Nilsen, J. E. Ø.: Large-scale atmospheric circulation variability and its impacts on the Nordic Seas climate, in: The Nordic Seas, An Integrated Perspective, Geophys. Monogr. Ser., Vol. 158, edited by: Drange, H., Dokken, T., Furevik, T., Gerdes, R., and Berger, W., AGU, Washington DC, 105–136, 2005.

Gascard, J.-C., Richez, C., and Rouault, C.: New insights on large-scale oceanography in Fram Strait: the West Spitsbergen Current, in Arctic Oceanography: Marginal Ice Zones and Continental Shelves, Geophys. Monogr. Ser., Vol. 49, edited by: Smith, W. O. and Grebmeier, J. M., AGU, Washington DC, 131–182, 1995.

Gray, L. J., Beer, J., Geller, M., Haigh, J. D., Lockwood, M., Matthes, K., Cubasch, U., Fleitmann, D. Harrison, G., Hood, L., Luterbacher, J., Meehl, G. A., Shindell, D., van Geel, B., and White, W.: Solar influences on climate, Rev. Geophys., 48, 1–53, RG4001, doi:10.1029/2009RG000282, 2010.
GWP: Jan Mayen, Global Volcanism Program, available at: www.volcano.si.edu/volcano.cfm?vn=376010 (last access: January 2015), 2014.
Haigh, J.: Solar variability and the Stratosphere, in: The Stratosphere: Dynamics, Transport and Chemistry, Geophys. Monogr. Ser., Vol. 190, edited by: Polvani, L. M., Sobel, A. H., and Waugh, D. W., AGU, Washington DC, 173–187, 2010.
Harold, J. M., Bigg, G. R., and Turner, J.: Mesocyclone activity over the Northeast Atlantic, Part 1: Vortex distribution and variability, Int. J. Climatol., 19, 1187–1204, 1999a.
Harold, J. M., Bigg, G. R., and Turner, J.: Mesocyclone activity over the Northeast Atlantic, Part 2: An investigation of causal mechanisms, Int. J. Climatol., 19, 1283–1299, 1999b.
Høyer, J. L., Karagali, I., Dybkjær, G., and Tonboe, R.: Multi sensor validation and error characteristics of Arctic sea surface temperature observations, Remote Sens. Environ., 212, 335–346, 2012.
Hurrell, J. W. and Deser, C.: North Atlantic climate variability: the role of the North Atlantic Oscillation, J. Marine Syst., 78, 28–41, 2009.
Hurrell, J. W., Kushnir, Y., Ottersen, G., and Visbeck, M. (Eds.): An overview of the North Atlantic Oscillation, in: The North Atlantic Oscillation: Climatic Significance and Environmental Impact, Geophys. Monogr. Ser., Vol. 134, doi:10.1029/134GM01, AGU, Washington DC, 1–35, 2003.
Imsland, P.: The volcanic eruption on Jan Mayen, January 1985: interaction between a volcanic island and a fracture zone, J. Volcanol. Geoth. Res., 28, 45–53, 1986.
Ineson, S. and Scaife, A. A.: The role of the stratosphere in the European response to El Niño, Nat. Geosci., 2, 32–36, doi:10.1038/ngeo381, 2009.
Ineson, S., Scaife, A. A., Knight, J. R., Manners, J. C., Dunstone, N. J., Gray, L. J., and Haigh, J. D.: Solar forcing of winter climate variability in the Northern Hemisphere, Nat. Geosci., 4, 753–757, 2011.
Johannessen, J. A., Johannessen, O. M., Svendsen, E., Shuchman, R., Manley, T., Campbell, W. J., Josberger, E. G., Sandven, S., Gascard, J. C., Olaussen, T., Davidson, K., and van Leer, J.: Mesoscale eddies in the Fram Strait marginal ice zone during the 1983 and 1984 Marginal Ice Zone experiments, J. Geophys. Res., 92, 6754–6772, 1987.

OSD
12, 103–134, 2015
Atmosphere–ocean interactions in the Greenland Sea
P. E. Binns

Kodera, K.: Solar cycle modulation of the North Atlantic Oscillation: implications in the spatial structure of the NAO, Geophys. Res. Lett., 29, 1218, doi:10.1029/2001GL014557, 2002.
Kodera, K.: Solar influence of the spatial structure of the NAO during winter 1900–1999, Geophys. Res. Lett., 30, 1175–1178, doi:10.1029/2002GL016584, 2003.
Kodera, K. and Kuroda, Y.: A possible mechanism of solar modulation of the spatial structure of the North Atlantic Oscillation, J. Geophys. Res., 110, D02111, doi:10.1029/2004JD005258, 2005.
Kolstad, E. W., Bracegirdle, T. J., and Seierstad, I. A.: Marine cold-air outbreaks in the North Atlantic: temporal distribution and associations with large-scale atmospheric circulation, Clim. Dynam., 33, 187–197, doi:10.1007/s00382-008-0431-5, 2009.
Kuroda, Y., Yamazaki, K., and Shibata, K.: Role of ozone in the solar cycle modulation of the North Atlantic Oscillation, J. Geophys. Res., 113, D14122, doi:10.1029/2007JD009336, 2008.
Laterius, K. and Quadfasel, D.: Seasonal to inter-annual variability of temperature and salinity in the Greenland Sea Gyre: heat and freshwater budgets, Tellus A, 62, 497–515, 2010.
NASA: Ocean Temperature, available at: https://podaac.jpl.nasa.gov (Dataset Discovery), last access: January 2015.
NERC: NERC Satellite Receiving Station, Dundee University, Scotland, available at: www.sat.dundee.ac.uk (last access: January 2015), 2013.
NOAA: available at: ftp://ftp.ngdc.noaa.gov/STP (last access: July 2013), 2011.
NOAA: Bathymetry, Marine Geology & Geophysics, GEODAS, available at: www.ngdc.noaa.gov (last access: January 2015), 2012.
Noer, G., Saetra, Ø., Lien, T., and Gusdal, Y.: A climatology study of polar lows in the Nordic Seas, Q. J. Roy. Meteorol. Soc., 137, 1762–1772, doi:10.1002/qj.846, 2011.
Reynolds, R. W. and Smith, T. M.: Improved global sea surface temperature analyses using optimum interpolation, J. Climate, 20, 929–948, 1994.
Reynolds, R. W., Smith, T. M., Liu, C., Chelton, D. B., Casey, K. S., and Schlax, M. G.: Daily high-resolution-blended analyses for sea surface temperature, J. Climate, 20, 5473–5496, 2007.
Reichler, T., Kim, J., Manzini, E., and Kröger, J.: A stratospheric connection to Atlantic climate variability, Nat. Geosci., 5, 783–791, doi:10.1038/Ngeo1586, 2012.
Rudels, B., Bjőrk, G., Nilsson, J., Winsor, P., Lake, I., and Nohr, C.: The interaction between waters from the Arctic Ocean and the Nordic Seas north of Fram Strait and along the East

OSD
12, 103–134, 2015
Atmosphere–ocean interactions in the Greenland Sea
P. E. Binns

Greenland Current: results from the Arctic Ocean-02 Oden expedition, J. Marine Syst., 55, 1–30, 2004.
Scaife, A. A., Knight, J. R., Vallis, G. K., and Folland, C. K.: A stratospheric influence on the winter NAO and North Atlantic surface climate, Geophys. Res. Lett., 32, L18715, doi:10.1029/2005GL023226, 2005.
Scaife, A. A., Ineson, S., Knight, J. R., Kodera, K., and Smith, D. M.: A mechanism for lagged North Atlantic climate response to solar variability, Geophys. Res. Lett., 40, 434–439, L18715, doi:10.1029/2005GL023226, 2013.
Schauer, U., Beszczynska-Möller, A., Walczowski, W., Fahrbach, E., Piechura, J., and Hansen, E.: Variation of measured heat flow through the Fram Strait between 1997 and 2006, in: Arctic-Subarctic Ocean Fluxes, edited by: Dickson, R., et al., Springer Science and Media B. V., Dordrecht, 65–85, 2008.
Serreze, M. C. and Barry, R. G.: The Arctic Climate System, Cambridge University Press, 2005.
Smedsrud, L. H., Sirevaag, A., Kloster, K., Sorteberg, A., and Sandven, S.: Recent wind driven high sea ice area export in the Fram Strait contributes to Arctic sea ice decline, The Cryosphere, 5, 821–829, doi:10.5194/tc-5-821-2011, 2011.
Sorteberg, A. and Walsh, J. E.: Seasonal cyclone variability at 70° N and its impact on moisture transport into Arctic, Tellus A, 60, 570–586, doi:10.1111/j.1600-0870.2008.00314.x, 2008.
Sorteberg, A., Kvamstø, N. G., and Byrkjedal, Ø.: Wintertime Nordic Seas cyclone variability and its impact on oceanic volume transports into the Nordic Seas, in: The Nordic Seas, An Integrated Perspective, Geophys. Monogr. Ser., Vol. 158, edited by: Drange, H., Dokken, T., Furevik, T., Gerdes, R., and Berger, W., AGU, Washington DC, 137–156, 2005.
Timmermans, M.-L., Proshutinsky, A., Ashik, I., Beszczynska-Moeller, A., Carmack, E., Frolov, I., Ingvaldsen, R., Itoh, M., Jackson, J., Kawaguchi, Y., Kikuchi, T., Krishfield, R., McLaughlin, F., Loeng, H., Nishino, S., Pickart, R., Rabe, B., Rudels, B., Semiletov, I., Schauer, U., Shakhova, N., Shimada, K., Sokolov, V., Steele, M., Toole, J., Weingartner, T., Williams, W., Woodgate, R., Yamamoto-Kawai, M., and Zimmermann, S.: Ocean, in: Arctic Report Card 2012, available at: http://www.arctic.noaa.gov/reportcard (last access: January 2015), 2012.
Trauth, M.: MATLAB Recipes for Earth Sciences, 2nd Edn., Springer, 2007.
Tsukernik, M., Deser, C., Alexander, M., and Tomas, R.: 2009. Atmospheric forcing of Fram Strait sea ice export: a closer look, Clim. Dynam., 35, 1349–1360, doi:10.1007/s00382-009-0647-z, 2009.

OSD
12, 103–134, 2015

Atmosphere–ocean interactions in the Greenland Sea

P. E. Binns

van Angelen, J. H., van den Broeke, M. R., and Kwok, R.: The Greenland Sea Jet: a mechanism for wind-driven sea ice export through the Fram Strait, Geophys. Res. Lett., 38, L12805, doi:10.1029/2011GL047837, 2011.
Visbeck, M. E., Chassignet, P., Curry, R. G., Delworth, T. L., Dickson, R. R., and Krahmann, G.: The ocean's response to North Atlantic Oscillation variability, in: The North Atlantic Oscillation: Climatic Significance and Environmental Impact, Geophys. Monogr. Ser., Vol. 134, edited by: Hurrell, J. W., Kushnir, Y., Ottersen, G., and Visbeck, M., AGU, Washington DC, 143–145, 2003.
Voet, G., Quadfasel, D., Mork, K. A., and Søiland, H.: The mid-depth circulation of the Nordic Sea derived from profiling float observations, Tellus A, 62, 516–529, 2010.
Wanner, H., Brönnimann, S., Casty, C., Gyalistras, D., Luterbacher, J., Schmutz, C., Stephenson, D. B., and Xoplaki, E.: North Atlantic Oscillation – concepts and studies, Surv. Geophys., 22, 321–382, 2001.

OSD
12, 103–134, 2015
Atmosphere–ocean interactions in the Greenland Sea
P. E. Binns

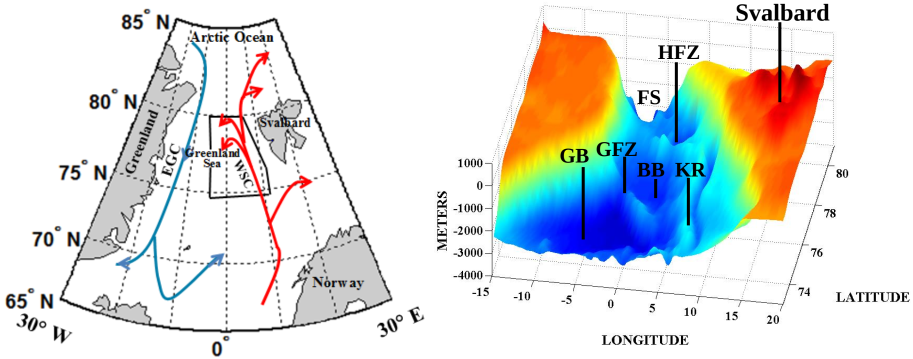

Figure 1. Locations. **(a)** The Nordic Seas with study area outlined. Atlantic Water flows northwards into the West Spitsbergen Current (WSC, red). Polar Water flows out of the Arctic into the East Greenland Current (EGC, blue). **(b)** Bathymetry of the Greenland Sea and Fram Strait (NOAA, 2012). FS – Fram Strait, KR – Knipovich Ridge, GB – Greenland Basin, GFZ – Greenland Fracture Zone, BB – Boreas Basin, HFZ – Hovgaard Fracture Zone.

OSD
12, 103–134, 2015

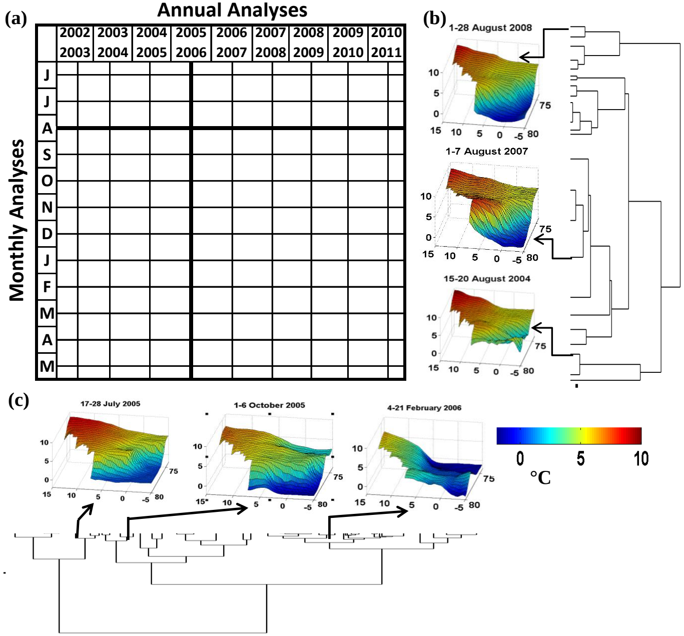

Figure 2. Cluster analysis methodology and representative sea surface temperature fields. An explanation of cluster analysis is given in the appendix. The objects in the analyses are daily sea surface temperature fields. **(a)** One set of analyses ("annual analyses", vertical lines) was made for each June–May period from June 2002 to May 2011. A second set ("monthly analyses", horizontal lines) was made for each month. **(b)** The monthly analysis for Augusts. The isometric plots are mean sea surface temperature fields of the clusters indicated, viewed from the north. High temperatures in the southeast indicate the inflowing Atlantic Water of the West Spitsbergen Current; the low temperatures in the northwest indicate Polar Water. Vertical axes: °C; horizontal axes: latitude and longitude. **(c)** As **(b)** but for the annual analysis for contrasting summer, autumn and winter clusters in 2005–2006. Note the lower temperatures in the southwest during October and February.

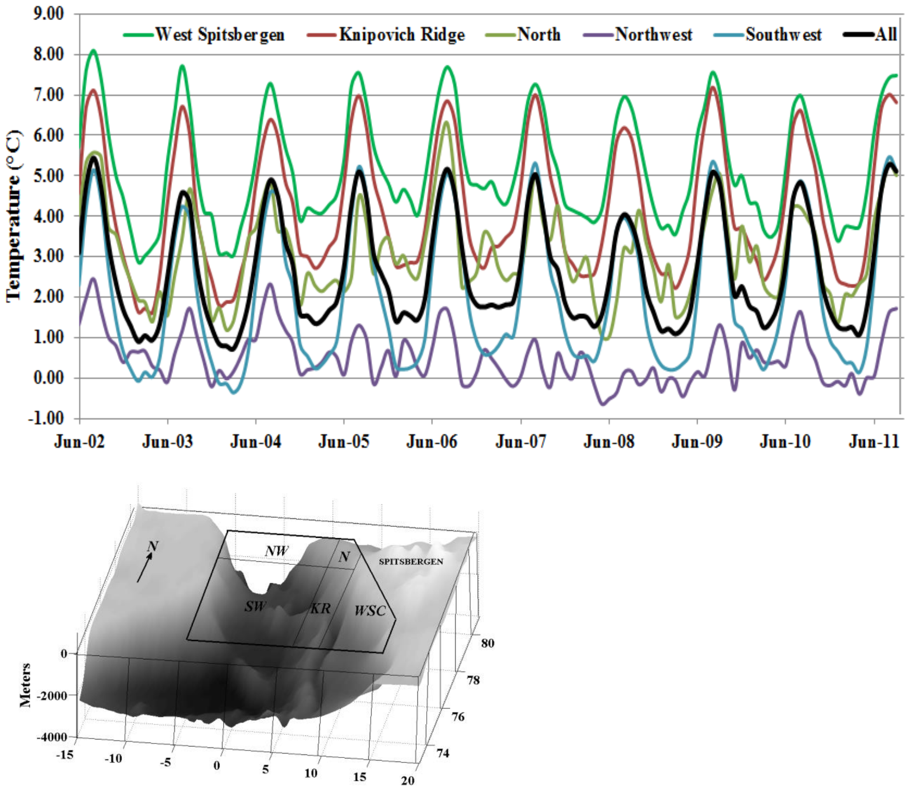

Figure 3. Monthly mean sea surface temperatures over the whole study area and within the sectors shown in the inset, June 2002 to September 2011 (NASA, 2002–2011). Temperatures of individual sectors broadly track, with the exception of the northwest sector, with its influx of Polar Water. Temperatures in the area as a whole increased from 2003 to 2006–2007, before decreasing in 2008, which stands out as the coldest year.

OSD
12, 103–134, 2015
Atmosphere–ocean interactions in the Greenland Sea
P. E. Binns

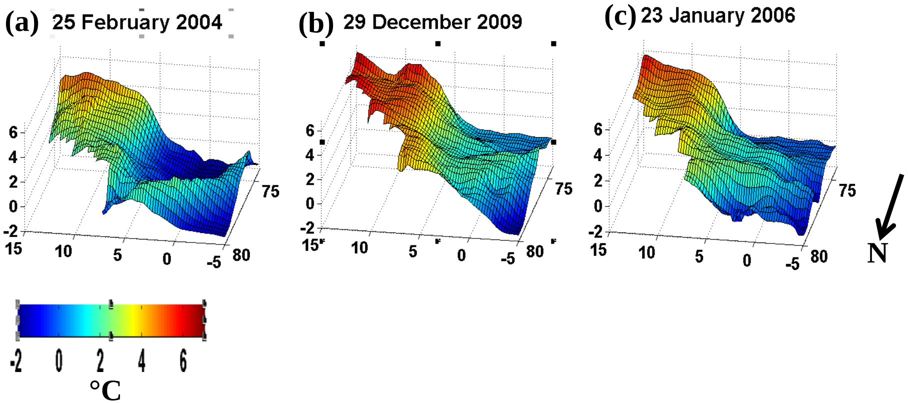

Figure 4. Winter sea surface temperature fields, chosen to represent three typical interactions in winter between recirculating Atlantic Water and Polar Water. Views from the north; vertical axes temperature (°C); horizontal axes latitude and longitude. Inflowing, warm Atlantic Water is apparent in the southeast. **(a)** Simple recirculation of warm Atlantic Water, which appears as a "ridge" with colder water on either side. **(b)** East–west trending features, interpreted as eddies "interfering" with recirculating Atlantic Water. **(c)** East–west trending features dominant.

OSD
12, 103–134, 2015

(a)

	2002 2003	2003 2004	2004 2005	2005 2006	2006 2007	2007 2008	2008 2009	2009 2010	2010 2011	2011	Avg.
Jun	11.6	9.4	12.1	13.1	12.5	9.6	9.2	10.6	10.5	10.9	11.0
Jul	13.4	10.7	14.8	15.1	14.2	10.0	9.2	12.1	10.2	10.2	12.0
Aug	14.2	14.5	14.6	14.4	14.0	10.0	9.9	10.2	13.0	10.4	12.5
Sep	13.6	14.8	11.1	14.1	13.5	9.8	11.9	12.0	9.9	11.5	12.2
Oct	13.2	13.9	12.3	16.2	12.8	14.1	14.2	13.8	13.0		13.7
Nov	11.5	13.1	15.0	15.1	16.3	14.0	14.2	12.7	14.1		14.0
Dec	15.1	15.1	17.9	15.4	16.8	14.6	13.9	14.6	15.9		15.5
Jan	15.1	16.9	16.3	20.5	15.9	14.6	14.8	13.0	13.9		15.7
Feb	16.8	13.7	18.3	15.7	13.3	17.2	13.3	11.6	13.8		14.9
Mar	14.5	15.9	13.8	17.3	12.5	11.9	13.5	12.6	18.9		14.5
Apr	13.0	12.3	12.9	12.9	12.2	10.0	11.3	12.5	13.3		12.3
May	9.8	11.3	10.9	12.1	9.2	7.2	10.1	9.9	9.0		9.9
Avg.	13.5	13.5	14.2	15.2	13.6	11.9	12.1	12.1	13.0		

SSN 10-20 | SSN <10 | Boreal Night

Scales on the right and on the base are gradational from red (high values) to blue (low values).

(b)

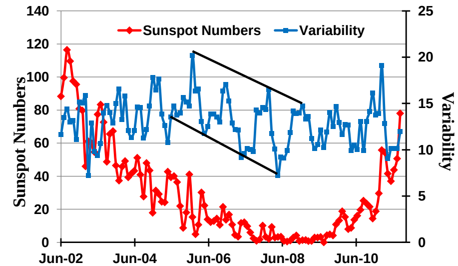

Figure 5. Comparison of sunspot numbers and the day-to-day variability of the sea surface temperature field (monthly means). **(a)** The lowest variability occurs in the summer months and in years with the lowest levels of solar activity. Months outlined in bold type indicate the start of tracking of temperature and variability (see Fig. 7). **(b)** Comparison of sunspot numbers and variability time series. Between 2005 and 2008, as solar activity decreases, the winter high and the spring low variability values also decrease, paralleling the decrease in sunspot numbers.

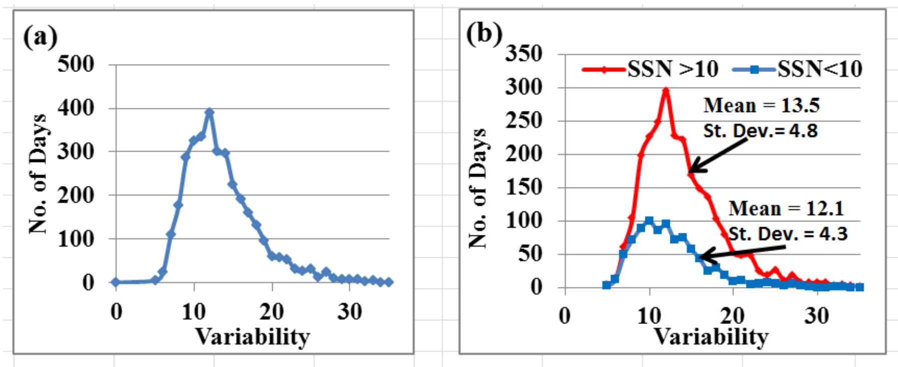

Figure 6. Frequency distributions, day-to-day variability of the SST fields. **(a)** All days. **(b)** Days separated into two groups, according to months with sunspot numbers below 10 (884 values) and above 10 (2525 values).

OSD
12, 103–134, 2015

Atmosphere–ocean interactions in the Greenland Sea

P. E. Binns

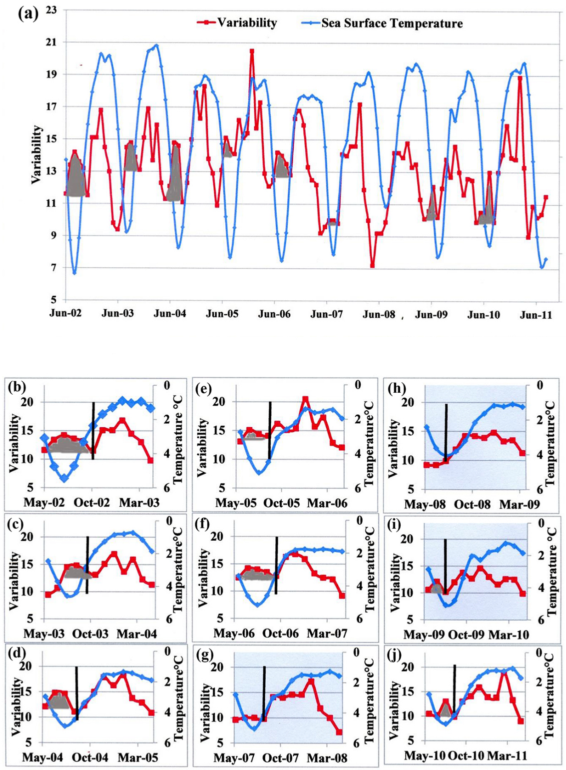

Figure 7. Comparison of mean sea surface temperatures with the day-to-day variability of the sea surface temperature field (monthly means). **(a)** Time series with inverted temperature scale. Grey infill highlights a pre-cursor, indicating changing levels of day-to-day variability in July and August. **(b–j)** As **(a)** with annual detail enlarged. Vertical black line indicates time at which decreasing mean sea surface temperature and increasing variability start to track. Blue shading indicates periods with low solar activity. Daily values are shown in Supplement, p. 6.

OSD
12, 103–134, 2015

Atmosphere–ocean interactions in the Greenland Sea

P. E. Binns

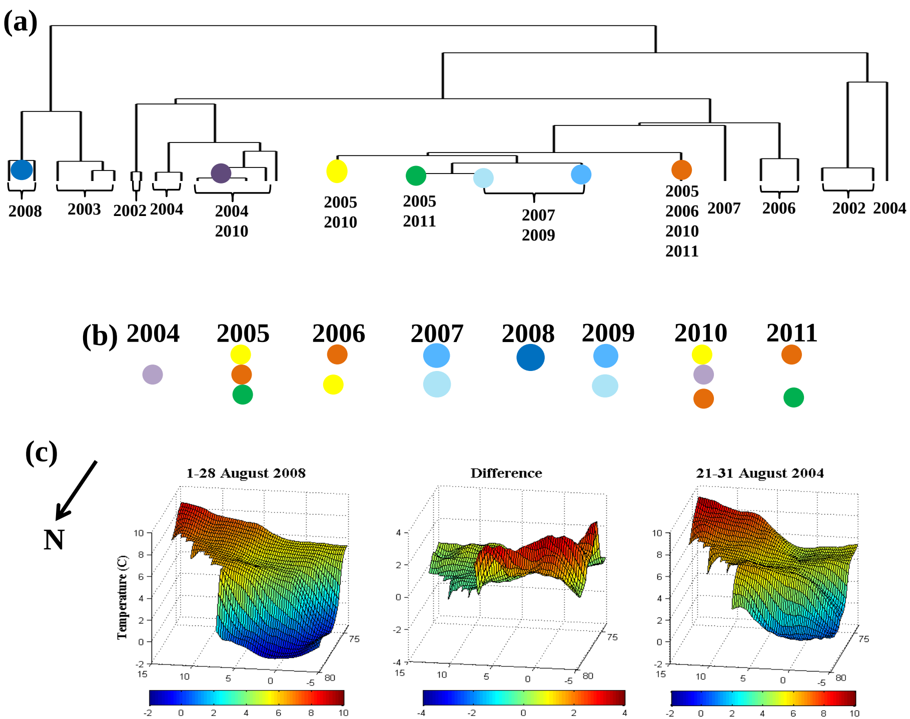

Figure 8. Symmetry of August sea surface temperature fields about 2007–2009, the years with lowest solar activity. **(a)** Dendrogram with clusters indicating symmetry depicted in colour, together with the years in which they have been detected. **(b)** Symmetry about 2007–2009. Clusters represented in blue shades have only been detected in these years. The mauve, yellow, green and brown clusters have only been detected in the years before and after. **(c)** Comparison of an August 2008 sea surface temperature field (left) with an August 2004 field (right). The difference field (centre) indicates higher 2004 temperatures in the northwest. View from north. Horizontal axes are latitude and longitude. (See also Supplement p. 7–11).

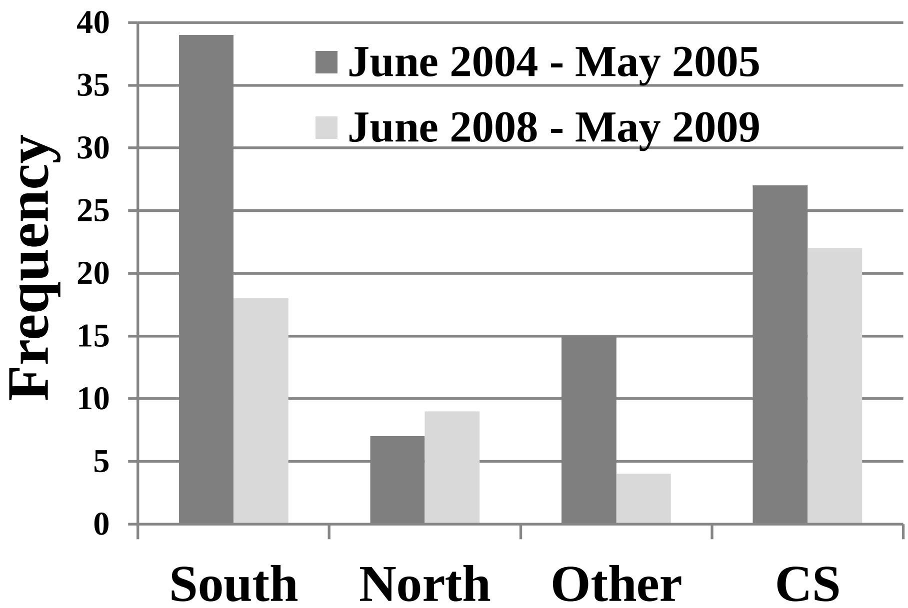

Figure 9. Comparison of cyclone systems in the Greenland Sea and their origin, during periods of relatively high (2004–2005) and low (2008–2009) solar activity. Also shown are the frequency of cold air outbreaks, indicated by cloud streets (CS).

OSD
12, 103–134, 2015

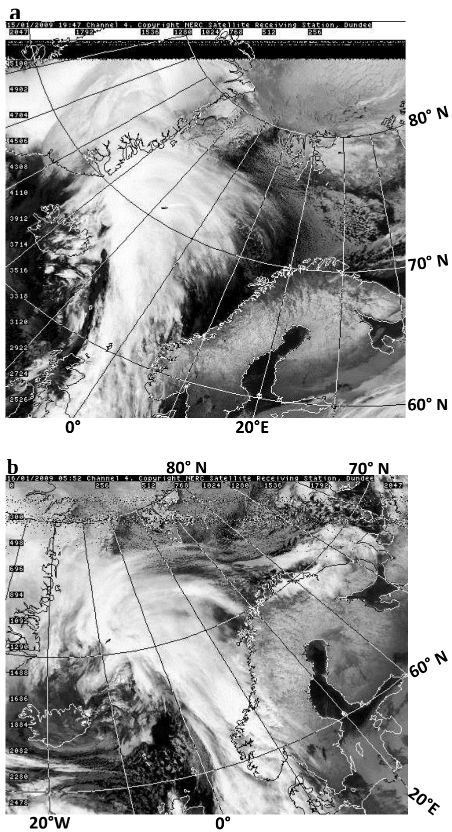

Figure 10. Infra-red AVHRR images showing a weather system moving northwestward across the Greenland Sea (NERC, 2013). **(a)** 15 January 2009 (19:47 UTC). The system approaches cloud streets to the southwest of Svalbard. **(b)** 16 January 2009 (05:52 UTC). Outlying clouds from the system appear to overlie the cloud streets.

OSD
12, 103–134, 2015

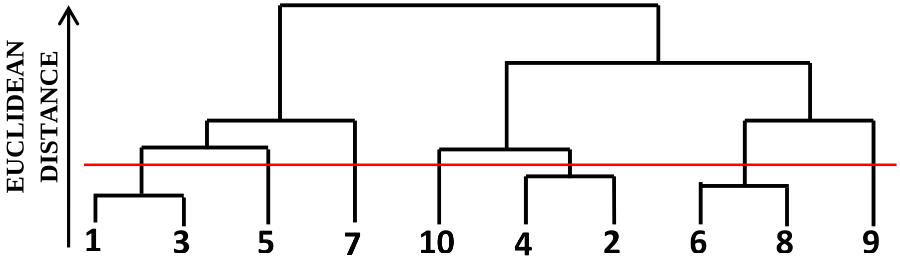

Figure A1. Simplified illustration of Cluster Analysis as used in this study. The clustering process is represented by a dendrogram. The numbers represent the daily SST fields. The analysis first finds the two fields which plot closest together in Euclidean space (here 1 and 3) and creates a new point midway between them. This is repeated for the next two pairs (4, 2 and 6, 8). The next closest points are 10 and the point created from 4 and 2; a new point is created from these. The process is repeated until all the points have been accounted for. A level in the dendrogram (the red line) is then arbitrarily selected so that a manageable number of clusters can be examined.

OSD
12, 103–134, 2015

Atmosphere–ocean interactions in the Greenland Sea

P. E. Binns